

687. Residual vibration reduction in low damping systems. Generation of regular piecewise algebraic polynomial inputs

J. M. Veciana, S. Cardona

Department of Mechanical Engineering, Universitat Politècnica de Catalunya
Barcelona 08028, Spain

E-mail: joaquim.maria.veciana@upc.edu

(Received 03 November 2011; accepted 4 December 2011)

Abstract. This paper presents a feedforward technique to generate command inputs to reduce residual vibration after transient maneuvers in mechanical systems. Synthesized inputs base their vibration reduction in zero-frequency content at the system resonances and are obtained taking advantage of the convolution theorem of the Fourier transform (FT). The analyzed systems are those that can be modeled as discrete linear systems with n vibratory degrees-of-freedom, and can be described with constant parameter motion equations. Although the complete cancellation of residual vibrations occurs for null damping ratios, the results obtained for low damped systems are quite acceptable. The method is particularized for rest-to-rest maneuvers and is compared to other literature methods. The new profiles present an optimal shape in terms of minimum acceleration fluctuation, which is useful to reduce the fatigue strength of the mechanical parts. By using a pulse as a base signal, the inputs obtained follow piecewise algebraic polynomial functions easily implementable through a B-spline scheme. The development includes a robust approach against the variation of the system parameters and a constraint determination aid for symmetric functions. Finally, some experimental results are presented using a two vibratory degrees-of-freedom test bed.

Keywords: residual vibration, residual response, vibration control, command shaping, input shaping, forcing function.

1. Introduction

Residual vibration reduction has been developed mainly in motion control systems. In those devices, fatigue of mechanical parts can be a drawback if the acceleration profile of the input shows excessive fluctuation during the transient. The main objective of the current development is to provide input functions, which present an optimal condition in terms of acceleration peak-valley counting compared to the standard literature methods. During the last 50 years a lot of work has been carried out within the methods based on feedforward techniques applied to discrete linear systems (Singhose [1]): some of them use time-domain approaches like signal generation by means of trigonometric series and command shaping through an impulse sequence; others use frequency-domain approaches, such as command conventional filtering and zero-placement.

Within the time-domain approaches, Aspinwall [2] defined point-to-point acceleration profiles, including the start and stop slopes, based on finite Fourier series expression. Those series were selected avoiding the system natural frequencies, and were compared with the classic profiles as rectangular pulse, double versine, and shaped pulse. Meckl and Seering [3, 4] demonstrated that for an undamped linear system with one non-forced vibratory degree-of-freedom, the spectral magnitude of the input at the system natural frequency is proportional to the amplitude of the residual vibration. They worked on forcing functions derived as a series expansion of ramped sinusoidal functions with coefficients chosen to minimize spectral magnitude at the system resonances, and proposed a method to provide robustness against

uncertainty of system modes. Chan and Stelson [5] compared some of the so-called s-curves such as raised cosine, piecewise parabolic and cubic input in different aspects, such as power, acceleration and jerk and developed a rescaling method to modify any fixed duration motion command to one of an arbitrary duration, while maintaining the property of having no residual vibration. Meckl et al. [6] proposed a method to select the ramp-up time in s-curves velocity profiles based on the frequency content of the forcing function, so that both the response time and the residual vibration amplitude are minimized.

Smith [7] was the first to propose the zero vibration (ZV) shaper: an input signal is shaped by convolving it with two impulses, properly located in time and with the appropriate amplitude. The vibration generated with the first one is suppressed with the vibration generated with the second one. This property remains invariable when any command signal is convolved with this impulse sequence. Singer and Seering [8] added a third impulse to individual sequences to provide robustness against possible variations of the system parameters – zero vibration and derivative (ZVD) shaper. Hyde and Seering [9] extended this method to multiple-mode systems. For n vibratory degree-of-freedom system, n impulse sequences are defined, each designed for each individual mode. The final impulse sequence used to shape the command signal is obtained by convolving all individual sequences in the time domain. Singhose et al. [10, 11] described a phasorial approach for the method described. For a three-impulse sequence, a method to adjust the relative angles between phasors – equivalent to the relative time delay between impulses – and their amplitudes was developed to reduce sensitivity to errors or variation of the system parameters. This approach is called the extra-insensitive shaper (EI). Singhose et al. [12] also reduced the transient time by adding negative impulses to the input sequence. Singh and Hepler [13] developed a variation of this method by designing an impulse sequence of two impulses in a non-robust case, or an impulse sequence of three impulses, in a more robust case, which cancels a so-called pseudo-mode with lower frequency than any of the system component modes. The resultant designed impulse train cancels all the higher frequency component modes and eliminates the vibration from the system.

Frequency-domain techniques have also been used to reduce the residual response. Singhose et al. [14] compared the input shapers with several types of conventional filters, properly designed to eliminate the system natural frequencies from the input signal. The analysis was carried out with FIR low-pass filters (Hamming, Parks-McClellan), IIR low-pass filters (Butterworth, Chebyshev, and elliptic), and notch filters derived from them. The results demonstrate that conventionally designed frequency-domain filters are less effective for command shaping than input shapers, which offer better performance in time response and lower levels of residual vibration.

Bhat and Miu [15] and Singh and Vadali [16] studied control strategies to accomplish precise point-to-point positioning of flexible structures, and demonstrated that the necessary and sufficient condition for zero residual vibration is that the Laplace Transform of the time-bounded control input should have zero contribution at the system poles. Murphy and Watanabe [17] and Tuttle and Seering [18] extended this zero-placement technique to the discrete domain, by constructing the impulse sequences in the z -plane for systems with any number of flexible modes.

In this paper, a Fourier transform based feedforward method is developed. Synthesized signals base their residual vibration reduction in a zero-frequency content at the system resonances. Although this is an analytically proven ZV method only for undamped systems, the results obtained for low damping systems are quite acceptable from a practical point of view. The method is particularized for rest-to-rest motion profiles with signals that follow simple piecewise low-order algebraic polynomial functions, which can be implemented easily through a B-spline scheme. The development includes a robust approach against the variation of the system parameters and a constraint determination aid for symmetric functions. Finally, some

experimental results are shown by using a two vibratory degrees-of-freedom test bed and the benefits of this development are validated.

2. Input design method

Meckl and Seering [4] demonstrated in the frequency domain that for an undamped linear system with one non-forced degree-of-freedom with vibratory behavior, the spectral magnitude of a transient input $u(t)$ at the system natural frequency f_0 is proportional to the amplitude of the residual vibration. Hence, for a null spectral magnitude, there is no residual vibration. Most of the symmetric functions (odd and even) present zero content at some determined frequencies, which is useful to use them for this purpose. The FT of a real even function $u(t)$ is also real and even, and its frequency spectrum is given by

$$U(f) = \text{FT}[u(t)] = \int_{-\infty}^{+\infty} u(t) \cos(2\pi ft) dt \quad (1)$$

In the case of a non-symmetric function, the magnitude of the frequency content can be described by

$$|U(f)| = \left| \int_{-\infty}^{+\infty} u(t) (\cos(2\pi ft) - j \sin(2\pi ft)) dt \right| \quad (2)$$

The magnitude of the frequency spectrum of a non-symmetric function is null when the real and the imaginary terms of (2) are zero at the same time, which is a more restricting condition than to cancel the magnitude of the former case (1). Practical examples show that almost all classical symmetric functions have zero-crossing points within their frequency spectra. Therefore, the use of such functions is recommended.

The demonstration stated by Meckl and Seering [4] can be described in the time domain: consider the generic system of the Fig. 1. Its motion equation is given by

$$(m_1 + m_2) \ddot{x} + c \dot{x} + kx = -m_2 \ddot{y}(t) \quad (3)$$

This expression can be rewritten as

$$\ddot{x} + 2\zeta(2\pi f_0) \dot{x} + (2\pi f_0)^2 x = -\frac{m_2}{m_1 + m_2} \ddot{y}(t) \quad (4)$$

where $f_0 = \sqrt{k/(m_1 + m_2)}/(2\pi)$ is the system natural frequency and $\zeta = c/(2\sqrt{(m_1 + m_2)k})$ is the damping ratio.

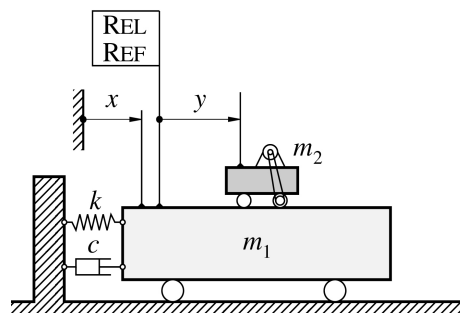


Fig. 1. Generic single-mode system

Consider that the impulse response of the system describes, for example, the velocity output \dot{x} for a unitary acceleration impulse $\ddot{y}(t) = \delta(t)$, and is given by the form

$$h(t) = C e^{-\zeta 2\pi f_d t} \cos(2\pi f_d t + \psi) \tag{5}$$

where C, f_d and ψ are respectively

$$C = -\frac{m_2}{m_1 + m_2} \frac{1}{\cos \psi} \tag{6}$$

$$f_d = f_0 \sqrt{1 - \zeta^2} \tag{7}$$

$$\psi = \arctan\left(\zeta / \sqrt{1 - \zeta^2}\right) \tag{8}$$

When $\zeta=0$ (undamped case), the indicated impulse response is given by $h(t) = C \cos(2\pi f_0 t)$. For a generic transient acceleration input $u(t) = \ddot{y}(t)$ defined between t_0 and t_f , the velocity output \dot{x} at t_f using the convolution integral is given by

$$\dot{x}(t_f) = \int_{t_0}^{t_f} u(\tau) C \cos(2\pi f_0(t_f - \tau)) d\tau \tag{9}$$

and the displacement is given by

$$x(t_f) = \int_{t_0}^{t_f} u(\tau) C \frac{1}{2\pi f_0} \sin(2\pi f_0(t_f - \tau)) d\tau \tag{10}$$

By developing $\dot{x}(t_f)$, it can be obtained

$$\dot{x}(t_f) = C \left[\cos(2\pi f_0 t_f) \int_{t_0}^{t_f} u(\tau) \cos(2\pi f_0 \tau) d\tau + \sin(2\pi f_0 t_f) \int_{t_0}^{t_f} u(\tau) \sin(2\pi f_0 \tau) d\tau \right] \tag{11}$$

By introducing the FT $[u(t)]$ at f_0 described in (2), the expression (11) yields

$$\dot{x}(t_f) = C \cos(2\pi f_0 t_f) \operatorname{Re}[U(f_0)] - C \sin(2\pi f_0 t_f) \operatorname{Im}[U(f_0)] \tag{12}$$

If the frequency content of the input $u(t)$ is null at f_0 , both addends of expression (12) are null. The same can be obtained by developing $x(t_f)$. Therefore, if the state-variables \dot{x} and x are zero at t_f , and the input $\ddot{y}(t)$ is null at t_f , following the expression (4) the acceleration \ddot{x} is also zero, and hence, the system stops moving at the end of the transient excitation and remains stopped.

2. 1. Single-mode systems

The convolution theorem of the FT states that under suitable conditions, the convolution of two signals in one domain (e.g., time domain) is equivalent to the product in the other domain (e.g., frequency domain), i.e., $\operatorname{TF}[u_1(t) \otimes u_2(t)] = U_1(f) \cdot U_2(f)$. The design method developed in this study consists of deriving input functions by means of convolving several transient signals in the time domain, which have the appropriate zero-crossing points in the frequency domain. For single-mode systems, only one of these signals is required to have a zero-crossing point at the natural frequency f_0 . In this case, the rectangular pulse is chosen as the base signal. As shown in Fig. 2, a first pulse $u_1(t)$ is defined with an arbitrary amplitude A_1 and a duration

$t_1=1/f_0$. The magnitude of the frequency spectrum is given by the expression (13) and is presented in the figure as well.

$$|U_1(f)| = A_1 \left| \frac{\sin(\pi f / f_0)}{\pi f} \right| \tag{13}$$

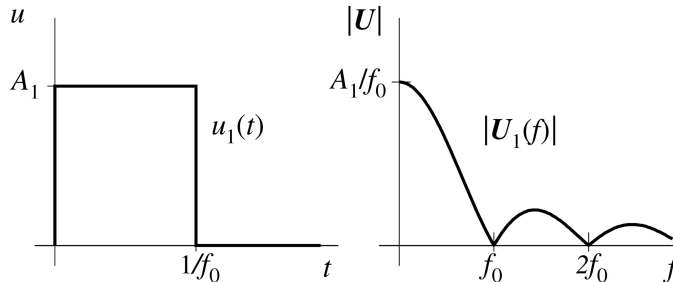


Fig. 2. Rectangular pulse and its magnitude in the frequency domain

In a general case, the profiles obtained should handle some functional requirements or constraints, like velocity increment or total displacement. The duration of the pulse is determined with the natural frequency of the system; therefore, only one constraint can be fixed, by modifying the amplitude A_1 of the pulse. To fix another constraint, the input $u(t)$ is obtained by convolving $u_1(t)$ with another rectangular pulse $u_2(t)$, with a duration t_2 and an arbitrary amplitude. The resultant function has a trapezoidal shape with a total duration of $1/f_0+t_2$, and amplitude A (Fig. 3). Thus, it is possible to accomplish both requirements, fixing the values A and t_2 . The frequency spectrum $U(f)$, which is given by the product of both frequency spectra $U_1(f)$ and $U_2(f)$, remains null at f_0 . If a null integral profile is desired, then $u(t)$ can be obtained by convolving the first rectangular pulse $u_1(t)$ with an odd transient signal $u_2(t)$ (Fig. 4). It can be noted that those points where the frequency content is null remain invariant with the integrals or derivatives of the function, provided that they exist.

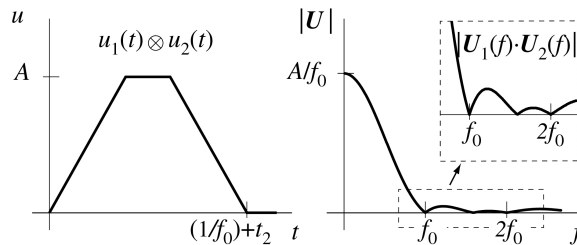


Fig. 3. Convolution of two rectangular pulses, $u_1(t)$ and $u_2(t)$

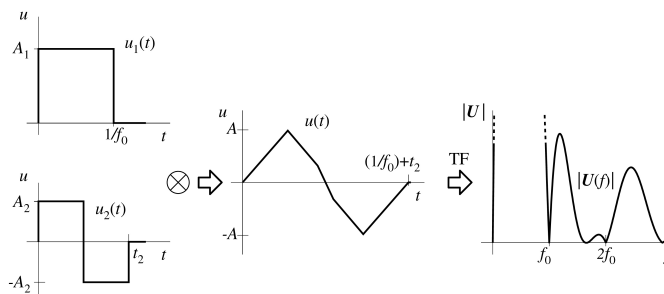


Fig. 4. $u(t)$ with a null integral profile

2. 2. Constraint determination aid for symmetric functions

In some cases, an iterative integration of the profile is needed to fix the desired constraints. In this context, it is presented in this subsection an easy way to calculate them by taking advantage of the functions symmetry. It is proven below that two transient acceleration profiles defined between t_0 and t_f , with even symmetry relative to the ordinate axis $(t_0+t_f)/2$, and with the same initial and final velocities, cover the same distance during the transient. Consider that $\ddot{y}_p(t)$ and $\ddot{y}_q(t)$ satisfy the indicated requirements (Fig. 5).

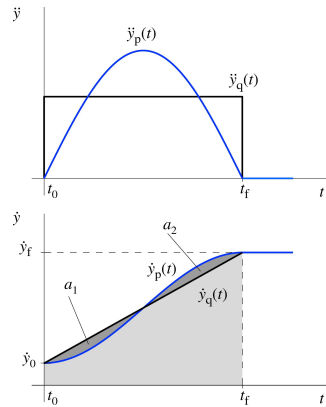


Fig. 5. Displacement equivalence between two acceleration profiles, $\ddot{y}_p(t)$ and $\ddot{y}_q(t)$, with even symmetry

Assume that the initial conditions of the motion are $\dot{y}_p(t_0) = \dot{y}_q(t_0) = \dot{y}_0$ and $y_p(t_0) = y_q(t_0) = y_0$. The velocity profiles can be described by

$$\dot{y}_p(t) = \dot{y}_0 + \int_{t_0}^t \ddot{y}_p(t) dt; \quad \dot{y}_q(t) = \dot{y}_0 + \int_{t_0}^t \ddot{y}_q(t) dt \quad (14)$$

The distances covered during the transient are given by

$$y_p(t_f) - y_0 = \int_{t_0}^{t_f} \left[\dot{y}_0 + \int_{t_0}^t \ddot{y}_p(t) dt \right] dt \quad (15)$$

$$y_q(t_f) - y_0 = \int_{t_0}^{t_f} \left[\dot{y}_0 + \int_{t_0}^t \ddot{y}_q(t) dt \right] dt$$

Therefore, the difference between the two distances covered is

$$y_p(t_f) - y_q(t_f) = \int_{t_0}^{t_f} \left[\int_{t_0}^t (\ddot{y}_p(t) - \ddot{y}_q(t)) dt \right] dt \quad (16)$$

By introducing the time coordinate of the symmetry axis, $(t_0+t_f)/2$, this expression yields

$$y_p(t_f) - y_q(t_f) = \int_{t_0}^{(t_0+t_f)/2} \left[\int_{t_0}^t (\ddot{y}_p(t) - \ddot{y}_q(t)) dt \right] dt + \int_{(t_0+t_f)/2}^{t_f} \left[\int_{t_0}^t (\ddot{y}_p(t) - \ddot{y}_q(t)) dt \right] dt \quad (17)$$

Even symmetry condition relative to the ordinate $(t_0+t_f)/2$ can be described by

$$\ddot{y}_p(t) = \ddot{y}_p(t_0 + t_f - t), \quad \ddot{y}_q(t) = \ddot{y}_q(t_0 + t_f - t) \quad (18)$$

By introducing it and changing the variable $\tau = t_0 + t_f - t$, the second term of expression (17) yields

$$\int_{(t_0+t_f)/2}^{t_0} \left[\int_{t_f}^{\tau} (\ddot{y}_p(\tau) - \ddot{y}_q(\tau)) d\tau \right] d\tau = \int_{(t_0+t_f)/2}^{t_0} \left[\int_{t_f}^{\tau_0} (\ddot{y}_p(\tau) - \ddot{y}_q(\tau)) d\tau + \int_{\tau_0}^{\tau} (\ddot{y}_p(\tau) - \ddot{y}_q(\tau)) d\tau \right] d\tau \quad (19)$$

As shown in Fig. 5, if the velocity at the end of the transient \dot{y}_f is the same for both maneuvers, therefore their difference is null

$$\dot{y}_p(t_f) - \dot{y}_q(t_f) = \int_{t_0}^{t_f} (\ddot{y}_p(t) - \ddot{y}_q(t)) dt = 0 \quad (20)$$

and, hence, the expression (19) can be rewritten as

$$\int_{(t_0+t_f)/2}^{t_0} \left[\int_{t_0}^{\tau} (\ddot{y}_p(\tau) - \ddot{y}_q(\tau)) d\tau \right] d\tau = - \int_{t_0}^{(t_0+t_f)/2} \left[\int_{t_0}^{\tau} (\ddot{y}_p(\tau) - \ddot{y}_q(\tau)) d\tau \right] d\tau \quad (21)$$

By introducing this term, the expression (17) yields

$$y_p(t_f) - y_q(t_f) = \int_{t_0}^{(t_0+t_f)/2} \left[\int_{t_0}^t (\ddot{y}_p(t) - \ddot{y}_q(t)) dt \right] dt - \int_{t_0}^{(t_0+t_f)/2} \left[\int_{t_0}^{\tau} (\ddot{y}_p(\tau) - \ddot{y}_q(\tau)) d\tau \right] d\tau \quad (22)$$

Both addends of expression (22) are the same and, hence, $y_p(t_f) - y_q(t_f) = 0$ which means that the distances covered by those profiles are the same. This conclusion can be graphically described by the equivalence of the areas a_1 and a_2 in Fig. 5. Therefore, the calculation of the functional requirements or constraints of a symmetric input can be easily done by making the equivalence to a simple symmetric profile, for example, to a rectangular pulse.

2. 3. Robustness

The frequency content of $u(t)$ in Fig. 3 grows quickly around the target frequency f_0 . The command input so defined could loose effectiveness owing to variations of the system parameters, which result in a displacement of its natural frequency f_0 . To provide robustness against these possible variations, it is proposed to reduce the magnitude of the frequency spectrum around f_0 , obtaining $u_1(t)$ by the convolution of two auxiliary pulses with the respective durations $1/f_0$ and p/f_0 ($p=1,2, \dots$), and arbitrary amplitudes. The magnitude of the frequency spectrum of the resultant signal is tangent with the abscises axis at the frequencies $f_0, 2f_0, 3f_0, \dots$ and is given by

$$|U_1(f)| = A_1 \left| \frac{\sin(\pi f / f_0) \sin(p\pi f / f_0)}{(\pi f)^2} \right| \quad p = 1, 2, \dots \quad (23)$$

To reduce the command duration, $p=1$ is recommended. Therefore, the shape of the signal becomes triangular (Fig. 6). As in the previous case, to include a second constraint, $u_1(t)$ is convolved with a rectangular pulse $u_2(t)$ with a duration t_2 and an arbitrary amplitude. The resultant signal $u(t)$ has a duration of $2/f_0+t_2$ (Fig. 7) and an amplitude A (both requirements can be accomplished by fixing t_2 and A) and is formed by five piecewise second-order (or less) algebraic polynomials (junction points marked with crosses in Fig. 7).

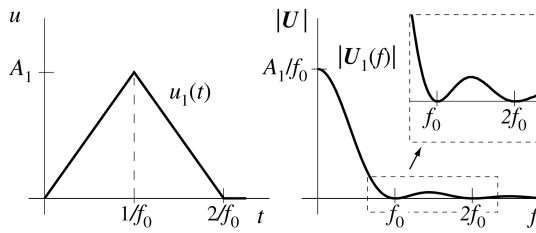


Fig. 6. Reduction in the frequency content around f_0 , by using a triangular signal $u_1(t)$

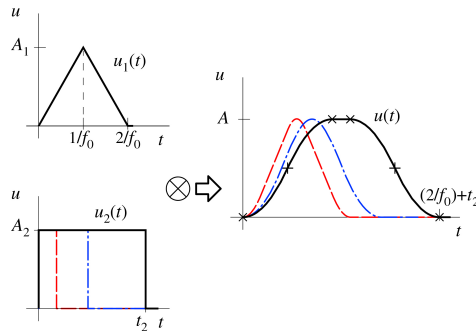


Fig. 7. Convolution of a triangular signal with various auxiliary rectangular pulses

To increase the bandwidth around f_0 , where the magnitude of the frequency spectrum is below a desired threshold g , it is possible to convolve more than two equal rectangular pulses. However, this implies longer command signals. To avoid this issue, it is proposed to slightly modify the durations of the two pulses used to obtain $u_1(t)$, changing $1/f_0$ by $1/(f_0+\Delta f)$ and $1/(f_0-\Delta f)$, with a small value of Δf . The resultant signal has a trapezium shape and, as shown in Fig. 8, the frequency bandwidth increases from a to b , in a similar way as in the method described by Singhose et al. [10, 11].

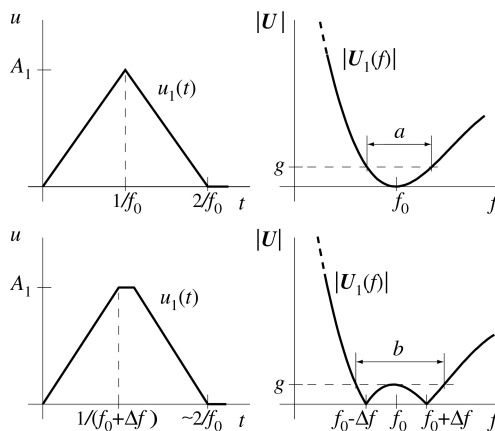


Fig. 8. Increment of useful bandwidth, by convolving to pulses with $1/(f_0+\Delta f)$ and $1/(f_0-\Delta f)$ durations

2. 4. Multiple-mode systems

For a generic n -mode vibratory system (Fig. 9), according to the modal decomposition theory and by using the velocity as the input and the acceleration as the output, the oscillatory term of an impulse response $h_{oi}(t)$ for the i -th coordinate x_i can be described by the form

$$h_{oi}(t) = \sum_{k=1}^n C_{ik} e^{-\zeta_k 2\pi f_{0k} t} \cos(2\pi f_{dk} t + \psi_{ik}) \quad (24)$$

where C_{ik} and ψ_{ik} are constants that depend on the system parameters, and f_{0k} , f_{dk} and ζ_k are, respectively, the natural frequency, the oscillation frequency and the damping ratio of the k -th mode. The oscillatory term of the impulse response for the undamped case is given by

$$h_{oi}(t) = \sum_{k=1}^n C_{ik} \cos(2\pi f_{0k} t) \quad (25)$$

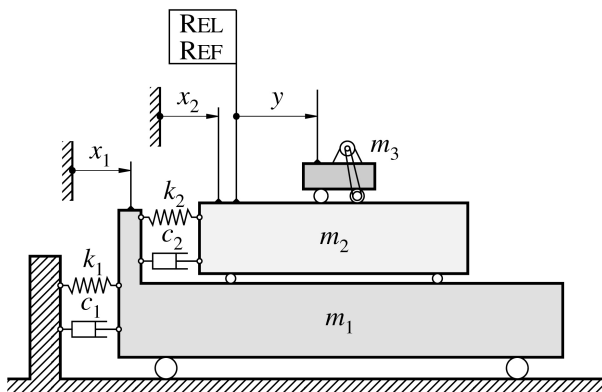


Fig. 9. Generic multiple-mode discrete linear system

Consider a generic transient acceleration input $u(t) = \ddot{y}(t)$ defined between t_0 and t_f . The velocity output \dot{x}_i at t_f is given by

$$\dot{x}_i(t_f) = \int_{t_0}^{t_f} u(\tau) h_{oi}(t - \tau) d\tau = \int_{t_0}^{t_f} u(\tau) \left[\sum_{k=1}^n C_{ik} \cos(2\pi f_{0k}(t - \tau)) \right] d\tau = \quad (26)$$

$$\sum_{k=1}^n C_{ik} \int_{t_0}^{t_f} u(\tau) \cos(2\pi f_{0k}(t - \tau)) d\tau$$

and the displacement x_i is given by

$$x_i(t_f) = \int_{t_0}^{t_f} u(\tau) \left[\sum_{k=1}^n C_{ik} \frac{1}{2\pi f_{0k}} \sin(2\pi f_{0k}(t - \tau)) \right] d\tau = \quad (27)$$

$$= \sum_{k=1}^n \frac{C_{ik}}{2\pi f_{0k}} \int_{t_0}^{t_f} u(\tau) \sin(2\pi f_{0k}(t - \tau)) d\tau$$

If the frequency content of the input $u(t)$ is null at $f_{01}, f_{02}, \dots, f_{0n}$, then the real and imaginary parts of expression (2) are zero at these frequencies, which indicates that the expressions (26) and (27) are null, following an analog development such as for single-mode systems. Therefore, the residual response is null because the state-variables x and \dot{x} are zero at t_f .

To generate the signal $u_1(t)$ that contains zero-crossing points at all the required system natural frequencies f_{0i} , it is proposed to convolve n rectangular pulses, each one with a duration of $1/f_{0i}$, and arbitrary amplitude. Consider that a system can be modeled with three vibratory modes with natural frequencies f_{01}, f_{02} , and f_{03} . The frequency spectrum of the resultant signal has zero-crossing points at those frequencies (Fig. 10). In the same way as for single-mode systems, to fix two constraints, the command input $u(t)$ is the result of the convolution of $u_1(t)$ with an auxiliary rectangular pulse $u_2(t)$. To provide robustness against system parameters variation, the techniques explained earlier can be used. However, the frequency content of this

type of signal diminishes significantly after the first natural frequency, and hence, generally it is adequate to use the non-robust approach.

The zero-crossing points of the signals obtained are located following a periodic basis of the inverse of the duration of the pulses involved. Sometimes, to reduce the duration of a multiple-mode input, it is worth using this property to obtain an approximation of a frequency f_{cmd} – the common maximum denominator of all the natural frequencies – or several of them, and use it to generate one auxiliary pulse replacing those for which the frequencies have been used to generate it. For the three-mode system of Fig. 10, the f_{cmd} should accomplish

$$\begin{aligned} f_{01} &\approx a f_{cmd} \\ f_{02} &\approx b f_{cmd} \\ f_{03} &\approx c f_{cmd} \end{aligned} \tag{28}$$

This approximation could be useful when the total duration of the signal using f_{cmd} is smaller than the duration of the signal using individual pulses, i.e., when $1/a + 1/b + 1/c > 1$.

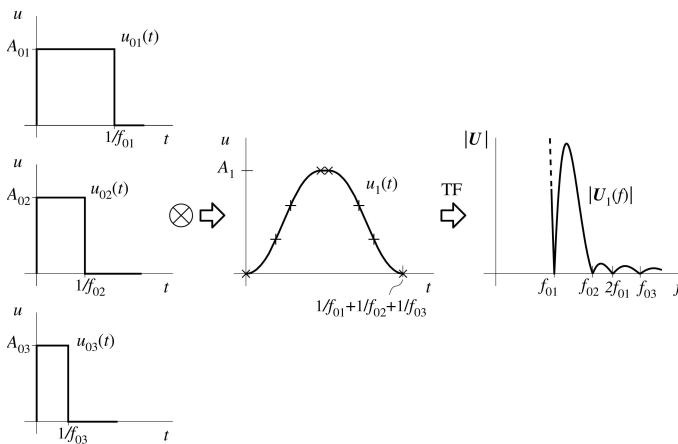


Fig. 10. Generation of $u_1(t)$ for a three-mode system

2. 5. B-spline scheme

A signal obtained by the convolution of m rectangular pulses is formed by piecewise $m-1$ or less order algebraic polynomials with a minimum guaranteed continuity degree of C^{m-2} within its definition range. These signals can be easily implemented through a non-parametric and non-rational B-spline scheme by the so-called node vector and control polygon, following the nomenclature detailed in Farin [21]. Fig. 11 illustrates an example of a motion profile generated for a single-mode system for the robust case. This curve was generated by the convolution of three pulses ($m=3$) and is formed by 5 different polynomials linked at the indicated crosses. Expressions (29) and (30) correspond respectively to the node vector u (expression (29)) and the control polygon ordinates d_i (expression (30)) that define entirely that curve. Other examples are illustrated in Veciana [19].

Node vector

$$u = \left\{ 0, 0, \frac{1}{f_0}, \frac{2}{f_0}, t_f - \frac{2}{f_0}, t_f - \frac{1}{f_0}, t_f, t_f \right\} \tag{29}$$

Control polygon ordinates

$$d = \{0, 0, A, A, A, 0, 0\} \tag{30}$$

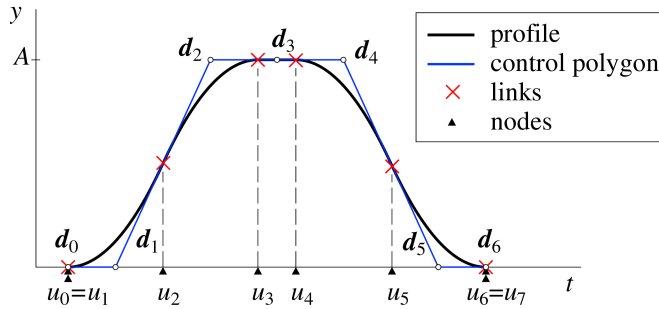


Fig. 11. B-spline scheme of a motion profile generated by the time-convolution of three pulses

3. Simulation results

3. 1. Acceleration fluctuation

The excessive oscillation in the acceleration profiles can result in a premature fatigue of the parts involved in the transmission of the system to be moved. To illustrate the benefits of the proposed technique to reduce the fatigue damage, some velocity profiles for rest-to-rest maneuvers were generated with a unitary displacement and assuming null initial conditions. The non-robust and robust cases were simulated:

1- Non robust case: The proposed technique defined by means of a pulse convolved with a trapezium was compared to the ZV shaper, considering an undamped single-mode system with a natural frequency of $f_0=1$ Hz. To obtain an overall input with the same maximum polynomial order and continuity (order 2 and continuity C^1 in this case) the unshaped function chosen for the ZV shaper was a smoothed-trapezium with the rising and falling sections defined by linked second order algebraic polynomials. The duration of these sections was defined to limit the acceleration to similar values than the proposed method and the duration of the overall input was fixed to four values between 1, 4 and 4 seconds. Fig. 12 shows the input velocities $\dot{y}(t)$ for the ZV shaper (a) and the proposed method (b), as well as the input accelerations $\ddot{y}(t)$ – where the acceleration fluctuation can be observed – and the system responses $x(t)$ where the residual vibration cancellation is shown.

2- Robust case: The proposed technique, defined now by a triangle convolved with a pulse, was compared to the ZVD shaper. The system and the unshaped function for the ZVD shaper follow the same criteria stated above. The duration of the overall input was fixed to four values between 2, 4 and 4 seconds (Fig. 13).

The acceleration profiles of the indicated figures show, in both cases, the benefits of using the proposed method regarding the fatigue damage cycle counting. While the maximum acceleration is approximately the same, the fatigue damage (number of acceleration peak-valley counts) is half in the proposed technique.

3. 2. Robustness comparison

A robustness comparison in percentage of residual vibration (PRV introduced by Singer and Seering [8], and Kozak et al. [20]) was performed by simulation. Standard methods such as ZV, ZVD and EI shapers with a 5% threshold were included and compared to the technique explained above. For the robust trapezium of the Fig. 8, a 5% threshold was used as well. The results are presented in Fig. 14. As it is shown in this figure, the robustness of a pulse is comparable to the ZV, and the triangle and the robust trapezium improves the results of the ZVD and EI, respectively.

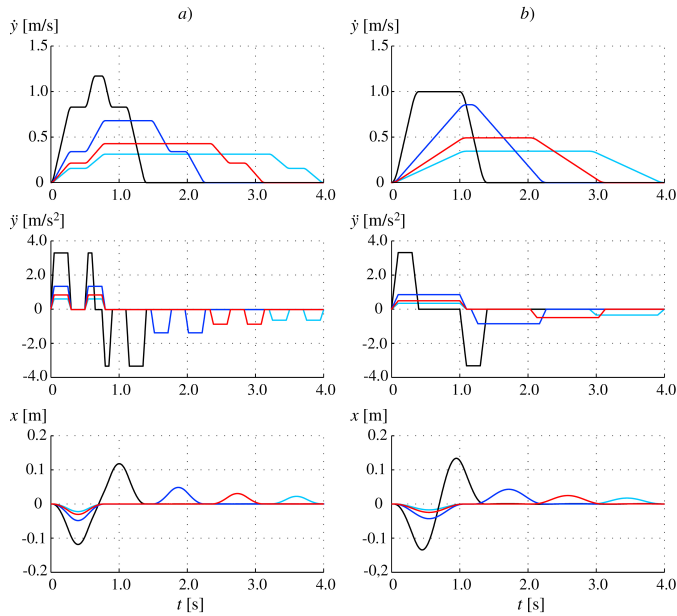


Fig. 12. Input velocity $\dot{y}(t)$, input acceleration $\ddot{y}(t)$ and system response $x(t)$ for the non-robust case: *a)* ZV shaper and *b)* proposed method

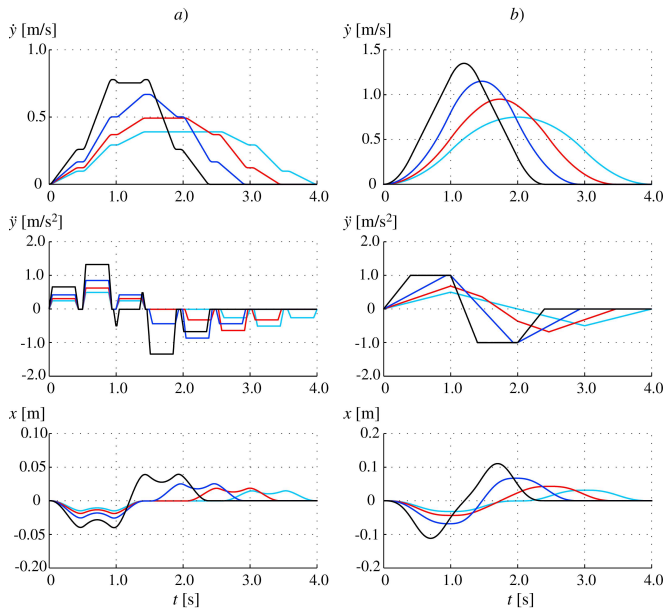


Fig. 13. Input velocity $\dot{y}(t)$, input acceleration $\ddot{y}(t)$ and system response $x(t)$ for the robust case: *a)* ZV shaper and *b)* proposed method

3. 3. Residual vibration in damped systems

Although the analytical cancellation of residual vibrations is stated for null damping ratios, the results obtained for low damped systems are usually acceptable. The percentage of residual vibration was analyzed for damped systems with damping ratios ζ of 0.1, 0.2 and 0.3. Fig. 15

shows this percentage versus the total input duration t_f when a trapezium was used (non-robust cancellation). Fig. 16 provides the robust case when a triangle was convolved with a pulse. In the former case, a 5% of residual vibration is not overcome for damping ratios $\zeta \leq 0,1$ and for durations over $1,4f_0$. For the robust case, less than 0,7% of residual vibration is expected for damping ratios $\zeta \leq 0,3$.

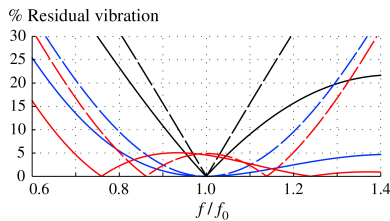


Fig. 14. Robustness comparison: ZV (dashed black), pulse (solid black), ZVD (dashed blue), triangle (solid blue), EI (dashed red) and robust trapezium (solid red)

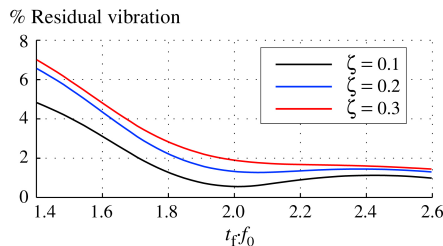


Fig. 15. Residual vibration versus the total input duration t_f for the indicated damping ratios when a trapezium is used (non-robust cancellation)

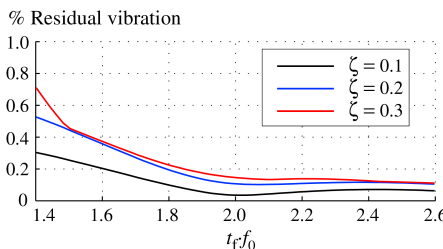


Fig. 16. Residual vibration versus the total input duration t_f for the indicated damping ratios when a smoothed trapezium is used (robust cancellation)

4. Experimental results

A test bed with three rotary degrees of freedom was built to check the adequacy of the method proposed. As shown in Fig. 17, it is made up by three coaxial rotary inertias. Two of them, I_1 and I_2 , have vibratory behavior owing to two rotational springs: one (k_2) assembled between inertias and the other (k_1) between the bottom inertia and the jig. The third inertia, I_3 , corresponds to the rotor of a direct current motor and its angular coordinate relative to I_2 is represented by φ_{rel} .

The motor follows a command input driven with a PI control and an incremental encoder. The absolute angular coordinates of the inertias I_1 and I_2 are φ_1 and φ_2 , respectively. Tangential accelerations of those inertias are measured by means of the two accelerometers shown in the figure. With respect to the damping ratios, as additional damping was not included, it can be

inferred that c_1 and c_2 are caused just by the internal frictions, and therefore, are expected to be low.

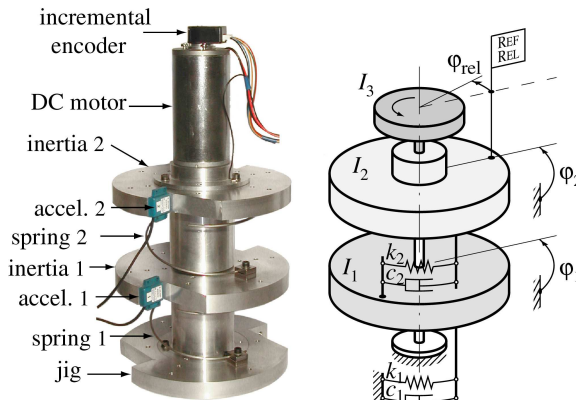


Fig. 17. Test bed with three rotary degrees of freedom and its equivalent discrete linear model

The test-bed setup gives two modes with natural frequencies at $f_{01}=1.2$ Hz and $f_{02}=3.4$ Hz, and with damping ratios $\zeta_{01}=0.012$ and $\zeta_{02}=0.013$. The bandwidths of the motor and the electronics should cover adequate margin of the system natural frequencies to avoid the filtering effect on the command input. The motor used in this application gives a frequency bandwidth of 9.1 Hz, and the electronic gives a frequency bandwidth of 2.5 kHz, thus both devices have values far enough from the system resonances.

The following is an example of several sets of velocity command inputs, $\dot{\phi}_{rel}$, that were tested, with all of them showing quite similar results. In each, three command inputs were designed: the first one is a single rectangular pulse that excites both modes with sufficient energy. The design of the second motion law is intended to reduce the residual vibrations from the higher mode, with the robust approach. The last one was designed to reduce the residual vibrations of both modes, with the non-robust methodology. In this example, an angular displacement of 680 radians and a transient duration of 1.9 s were fixed as the functional requirements. The output $\dot{\phi}_1(t)$ is presented in Fig. 18 (output $\dot{\phi}_2(t)$ is quite similar and hence, has been omitted): when the command input is a rectangular pulse, both modes can be observed in the residual vibration (output *a*). However, the higher mode component is reduced in the second case (output *b*). In the third case, almost no residual vibration is observed (output *c*). Quantifying this result, the first excitation gives a percentage of residual vibration (PRV) of 9.5 % and 2.2 % for the low and high modes, respectively. The PRV for the second input are 7.7 % and 0.2 % and 0.7 % and 0.05 % for the last one.

5. Conclusions

A feedforward method to design command inputs to reduce the residual vibration was developed in this paper. Linear motion equations with constant parameters were used to model the n degree-of-freedom vibratory systems. The motion profiles, generated by convolving symmetric transient functions in the time domain, base their residual vibration reduction on the cancellation of the frequency content at the system resonances. These frequency-domain zero-crossing points can be properly located by adjusting the duration of one of the functions convolved. By using a pulse as a base signal, the inputs obtained follow piecewise algebraic polynomial functions, easily implementable through a B-spline scheme. The development included a robust approach against the variation of the system parameters with results comparable to the ZVD and EI approaches, as well as a constraint determination aid for

symmetric functions. The new profiles presented an optimal shape in terms of minimum acceleration fluctuation compared to other literature methods, which is useful to reduce the fatigue strength of the mechanical parts. Although the development is a zero-vibration method analytically proven for undamped systems, an acceptable vibration reduction is obtained for damping ratios below 0.1 for the non-robust case and 0.3 for the robust one, assuming a 5% of PRV.

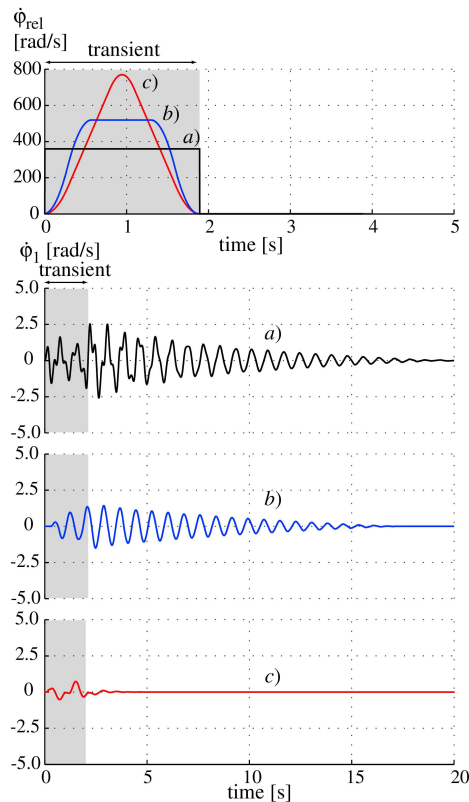


Fig. 18. Sample test outputs $\dot{\phi}_1(t)$ for the following inputs $\dot{\phi}_{rel}(t)$: a) rectangular pulse, b) reduction of the residual vibration from the higher mode (robust) and c) all-mode residual vibration reduction (non-robust)

References

- [1] **Singhose W. E.** Command Shaping for Flexible Systems: A Review of the First 50 Years. International Journal of Precision Engineering and Manufacturing, Vol. 10, Issue 4, 2009, p. 153 - 168.
- [2] **Aspinwall D. M.** Acceleration Profiles for Minimizing Residual Response. ASME Journal of Dynamic Systems, Measurement and Control, Vol. 102, Issue 2, 1980, p. 3 - 6.
- [3] **Meckl P. H., Seering W. P.** Minimizing Residual Vibration for Point-to-Point Motion. ASME Journal of Vibration, Acoustics, Stress and Reliability in Design, Vol. 107, Issue 1, 1985, p. 378 - 382.
- [4] **Meckl P. H., Seering W. P.** Reducing Residual Vibration in Systems with Time-Varying Resonances. IEEE International Conference on Robotics and Automation, Raleigh, NC, USA, Vol. 4, 1995, p. 1690 - 1695.
- [5] **Chan T. M., Stelson K. A.** Point-to-Point Motion Commands that Eliminate Residual Vibration. IEEE Proceedings of the American Control Conference, Seattle, WA, USA, Vol. 1, 1995, p. 909 - 913.

- [6] **Meckl P. H., Arestides P. B., Woods M. C.** Optimized S-Curves Motion Profiles for Minimum Residual Vibration. IEEE Proceedings of the American Control Conference, Philadelphia, PA, USA, Vol. 5, 1998, p. 2627 - 2631.
- [7] **Smith O. J. M.** Posicast Control of Damped Oscillatory Systems. Proceedings of the IRE, Vol. 45, Issue 9, 1957, p. 1249 - 1255.
- [8] **Singer N. C., Seering W. P.** Preshaping Command Inputs to Reduce System Vibration. ASME Journal of Dynamic Systems, Measurement and Control, Vol. 112, Issue 1, 1990, p. 76 - 82.
- [9] **Hyde J. M., Seering W. P.** Using Input Command Pre-Shaping to Suppress Multiple Mode Vibration. IEEE Proceedings of the International Conference on Robotics and Automation, Sacramento, CA, USA, Vol. 3, 1991, p. 2604 - 2609.
- [10] **Singhose W. E., Seering W. P., Singer N. C.** Shaping Inputs to Reduce Vibration: a Vector Diagram Approach. IEEE Proceedings of the International Conference on Robotics and Automation, Cincinnati, OH, USA, Vol. 2, 1990, p. 922 - 927.
- [11] **Singhose W. E., Seering W. P., Singer N. C.** Residual Vibration Reduction Using Vector Diagrams to Generate Shaped Inputs. ASME Journal of Mechanical Design, Vol. 116, 1994, p. 654 - 659.
- [12] **Singhose W. E., Seering W. P., Singer N. C.** Design and Implementation of Time-Optimal Negative Input Shapers. ASME Winter Annual Meeting, Chicago, IL, USA, 1994, p. 151 - 157.
- [13] **Singh T., Heppler G. R.** Shaped Input Control of a System with Multiple Modes. ASME Journal of Dynamic Systems, Measurement and Control, Vol. 115, Issue 3, 1993, p. 341 - 347.
- [14] **Singhose W. E., Singer N. C., Seering W. P.** Comparison of Command Shaping Methods for Reducing Residual Vibration. Proceedings of the European Control Conference, Rome, Italy, 1995, p. 1126 - 1131.
- [15] **Bhat S. P., Miu D. K.** Precise Point-to-Point Positioning Control of Flexible Structures. ASME Journal of Dynamic Systems, Measurement and Control, Vol. 112, Issue 4, 1990, p. 667 - 674.
- [16] **Singh T., Vadali S. R.** Robust Time - Delay Control. ASME Journal of Dynamic Systems, Measurement and Control, Vol. 115, Issue 2A, 1993, p. 303 - 306.
- [17] **Murphy B. R., Watanabe I.** Digital Shaping Filters for Reducing Machine Vibration. IEEE Transactions on Robotics and Automation, Vol. 8, Issue 2, 1992, p. 285 - 289.
- [18] **Tuttle T. D., Seering W. P.** A Zero-Placement Technique for Designing Shaped Inputs to Suppress Multiple-Mode Vibration. Proceedings of the American Control Conference, Baltimore, MD, USA, 1994, p. 2533 - 2537.
- [19] **Veciana J. M.** Reducció de Vibracions Residuals en Moviments Transitoris. Definició de Lleis de Moviment per Mitjà de Corbes B-spline. Ph. D. thesis, Universitat de Girona, Girona, Spain, 2007.
- [20] **Kozak K., Singhose W., Ebert-Uphoff I.** Performance Measures for Input Shaping and Command Generation. ASME Journal of Dynamic Systems, Measurement and Control, Vol. 128, Issue 1, 2006, p. 731 - 736.
- [21] **Farin G.** Curves and Surfaces for Computer-Aided Geometric Design. San Diego: Academic Press, Inc., 1997.